A Sensor-Actuator Map for Organization of Position Sensor Feedback Control for Multiple Links Structure / Wire Driven System

Hitoshi Kino
Faculty of Engineering
Fukuoka Institute of Technology
JAPAN, kino@fit.ac.jp

Shigeru Yabe
Ishikawajima-Harima Heavy
Industries Co., Ltd., JAPAN
shigeru_yabe@ihi.co.jp

Naoki Honjo and Sadao Kawamura
Faculty of Science and Engineering
Ritsumeikan University, JAPAN
kawamura@se.ritsumei.ac.jp

Abstract

Multiple Links Structure / Wire Driven (tendon) System is one of robot structures, that has a serial-link structure driven by a wire-drive mechanism. It can be applied to a manipulator like elephant's trunk, a moray arm, the backbone of a humanoid, etc.. However, transformations among coordinates (task-oriented, joint-angles and wire-length) are very complicated. Therefore, it is not clear how sensory feedback control laws should be realized for the system. In this paper, we propose a sensor-actuator map in which the sensor coordinates and actuator coordinates are arranged. By finding the paths from the sensor coordinates to the actuator coordinates on the map, the sensory feedback control laws can be built.

1 Introduction

A multiple links structure / wire driven system has links structure driven by wire tendons. Such a system already has been studied so far[1]. Also, we developed a force display device for virtual reality using a serial-link structure driven by a parallel-wire mechanism as shown in Fig. 1. Moreover, the wire driven systems using elastic hose instead of heavy rigid links have been applied to the backbone of a humanoid and flexible manipulators.

In the system, however, transformations among coordinates (task-oriented, joint-angles and wire-length) to represent the position-orientation of an end-effector are very complicated. Therefore, it is not clear how sensory feedback control laws should be realized for the system. In this paper, we propose a sensor-actuator map in which the coordinates are arranged. By finding the paths from the sensor coordinates to the actuator coordinates on the map, the sensory feedback control laws can be built. So it can visualize the control laws. The sensory feedback control for positioning, in brief, is to construct a signal of input in actuator coordinates from signals in sensor coordinates. Because a path on the map means transformation among coordinates, finding the paths on the map shows us what control laws can be realized for a multiple links structure / wire driven system.

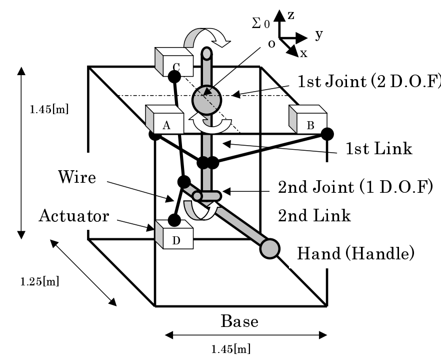

Figure 1. Serial-Link Structure Driven by Parallel-Wire Mechanism

2 Relations Among Vectors

2.1 An example of system

In this paper, we discuss with focusing on especially the serial-link structure driven by parallel-wire mechanism as shown in Fig. 1[2]. This system consists of a base, actuators, links and wires. Two very light links made of duralumin form a serial-link structure. As a whole, the serial-link structure achieves three D.O.F. motion (x,y,z) at the tip of the second link. Four wires in total, two wires attached on each link, achieve three D.O.F. motion of the serial-link structure. Since the wires can generate only tension, the system need such a redundant actuation[3]. Three encoders are set at each joint in order to measure angles of the joints. Each link has a counter weight so that the gravitational influence on the link is negligible. Four actuators, from A to D are arranged on the frame. An actuator consists of a reeling pulley, two gears, a small guiding pulley and a DC

Proceedings of the 18th International Conference on Advanced Information Networking and Application (AINA'04)
0-7695-2051-0/04 $ 20.00 © 2004 IEEE

servo motor (60[W]) with a rotary encoder to measure wire length.

2.2 Sensor-Actuator Map

PID positioning control of which system has plural coordinates like this system has not been organized well. In this subsection, we organize relations among vectors (displacement, velocity and force) of the coordinates (task-oriented, joint-angle and wire length), then visually express these relations using a map.

In the following, we assume that the serial-structure is not redundant, the hand has n_0 D.O.F. motions driven by totally m wires. Wires can generate only tension so that this system needs a redundant actuation, then $n_0 < m$. The robot is driven only by the wire tension. Gravitational influence can be ignored. At least, one kind of sensor is equipped to measure the displacement (the end-effector position, the joint-angles, the wire length).

The system has three displacement vectors as candidates that can be sensor input: the position vector of an end-effector $\boldsymbol{x} \in R^{n_0}$, a joint angle vector $\boldsymbol{\theta} \in R^{n_0}$ and a wire length vector $\boldsymbol{q} \in R^m$. These three vectors are called displacement vectors in this paper. Here, the following equations are obtained as kinematics if the relation among the displacement vectors can be calculated analytically,

$$\begin{array}{lll} \boldsymbol{x} = G_1(\boldsymbol{\theta}), & \boldsymbol{q} = G_2(\boldsymbol{x}), & \boldsymbol{\theta} = G_3(\boldsymbol{q}), \\ \boldsymbol{q} = G_4(\boldsymbol{\theta}), & \boldsymbol{x} = G_5(\boldsymbol{q}), & \boldsymbol{\theta} = G_6(\boldsymbol{x}), \end{array} \tag{1}$$

where the G_i ($i = 1 \ldots 6$) is the kinematical function that relates among the displacement vectors.

It is well-known that differentiation of the displacement relations described in Eqs. (1) yields the velocity relations given by Eqs. (2). In this paper, the vectors, $\dot{x}$, $\dot{\theta}$ and $\dot{q}$ are generically called velocity vectors.

$$\begin{array}{rcl} \dot{\boldsymbol{x}} & = & \boldsymbol{J_1}(\boldsymbol{\theta})\dot{\boldsymbol{\theta}}, \quad \dot{\boldsymbol{q}} = \boldsymbol{J_2}(\boldsymbol{x})\dot{\boldsymbol{x}}, \quad \dot{\boldsymbol{\theta}} = \boldsymbol{J_3}(\boldsymbol{q})\dot{\boldsymbol{q}}, \\ \dot{\boldsymbol{q}} & = & \boldsymbol{J_4}(\boldsymbol{\theta})\dot{\boldsymbol{\theta}}, \quad \dot{\boldsymbol{x}} = \boldsymbol{J_5}(\boldsymbol{q})\dot{\boldsymbol{q}}, \quad \dot{\boldsymbol{\theta}} = \boldsymbol{J_6}(\boldsymbol{x})\dot{\boldsymbol{x}}, \end{array} \tag{2}$$

where the matrix $\boldsymbol{J_i}$ implies the Jacobian matrix obtained from the function G_i. As long as the matrix J_i has full-rank, we can obtain the inverse relations of Eqs. (2) using the inverse matrix $\boldsymbol{J_i}^{-1}$ and the pseudo inverse matrix $\boldsymbol{J_i}^{+}$.

Next, consider force relations: the relations among a force-moment vector $f \in R^{n_0}$ generated at the end-effector, a torque vector $\tau \in R^{n_0}$ at the joints and a wire tension vector $\alpha \in R^m$. We call *force vectors* as the general term for these vectors in this paper. It is well-known that the relations can be obtained through the principle of virtual work from the velocity relations described by Eqs. (2). We can also obtain the inverse relation of the force relation as well as the velocity relation. The details are omitted in this paper because of space limitations. The transformations between

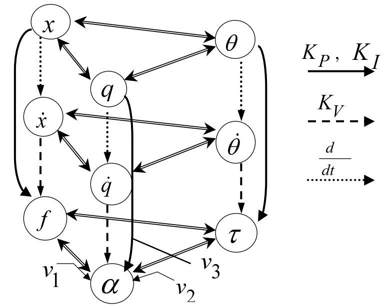

Figure 2. Sensor-actuator Map

vectors with different size cause internal force vectors that belong in the null space of the matrix.

We turn now to feedback transformations from the displacement vectors to the force vectors. The feedback terms based on the displacement error in each coordinates are described by

$$\begin{array}{rcl} \boldsymbol{\tau} & = & \boldsymbol{K_{P1}}(\boldsymbol{\theta_d} - \boldsymbol{\theta}), \qquad \boldsymbol{f} = \boldsymbol{K_{P2}}(\boldsymbol{x_d} - \boldsymbol{x}), \\ \boldsymbol{\alpha} & = & \boldsymbol{K_{P3}}(\boldsymbol{q_d} - \boldsymbol{q}) + \boldsymbol{v_3}, \end{array} \tag{3}$$

where $\boldsymbol{\theta_d}$, $\boldsymbol{x_d}$ and $\boldsymbol{q_d}$ are desired vectors. The matrix $\boldsymbol{K_{Pi}}$ is a gain matrix for the proportional feedback, and the vector $\boldsymbol{v_3}$ means the internal force. Since wire can generate only tension, to accomplish the positioning control scheme in the wire length coordinate needs the positive internal force ($\boldsymbol{v_3} > 0$) in order not to slack off the wire ropes. As well as P control terms, I and D terms that consist of PID feedback control are given.

As far as the velocity signal is concerned, today it is possible to obtain the velocity information from the displacement signals measured by the displacement sensors through difference of the signals because of infinitesimal sampling time.

After all, we have a whole map to indicate all relations among the vectors as shown in Fig. 2. This map is simplified for easily viewable, and called a *sensor-Aactuator map*. An arrow which means transformation between vectors is called a transfer arrow. Even though we have assumed that the relations among the displacement vectors can be analytically obtained, in practice it depends on hardware, modeling and so on. When it is applied to actual system, we do not enter transfer arrows of which relations can not be analytically obtained. Obtaining the displacement variable in the Jacobian matrix by using a sensor is one of the conditions to enter the transfer arrow on the map. The vector $\boldsymbol{v_i}$ in Fig. 2 means the internal force. In this paper, the α node that indicates actuator input is called the *actuator node*, the vector node directly measured by a sensor is called the *sensor node*. The node that means the origin of the feedback transformation is called the *feedback node*. In the next section, we will explain about the making paths to express PID feedback control laws.

Since each transfer arrow graphically shows the analytic relation between the vectors, making paths from the sensor node to the actuator node can express the actuator input of PID feedback control laws for a given system. Therefore, in order to consider PID feedback control laws for the system, at first we investigate if each transformation among the vectors is analytically realized or not. Then, preparing the sensor-actuator map makes the organization of PID control easy. So, the map is very useful in order to design control laws.

2.3 Converting from Path to Control Law

We clarify the relation between the paths obtained on the sensor-actuator map and investigate PID feedback control laws to converge the position vector $\boldsymbol{x}$ at the desired one, $\boldsymbol{x_d}$, and the velocity $\dot{\boldsymbol{x}}_{\boldsymbol{d}}$ at zero.

First, we consider proportion position control (P control) after the separation of PID control in order to simplify this discussion. Generally, P control is given by the following equation as actuator input,

$$\boldsymbol{\alpha_P} = \boldsymbol{J}\boldsymbol{K_P}\big(G_i(\boldsymbol{x_d}) - G_j(\boldsymbol{s})\big) + \boldsymbol{v}. \tag{4}$$

where $\boldsymbol{s} = \boldsymbol{x}$ or $\boldsymbol{q}$ or $\boldsymbol{\theta}$. The matrix $\boldsymbol{J}$ achieves the transformation from the feedback coordinate to wire tension, and the matrix $\boldsymbol{K_P}$ represents a gain matrix. The function $G_i(\boldsymbol{x_d})$ is the kinematics that transforms the desired position of the end-effector to the desired one in the feedback coordinate, and the function $G_j(\boldsymbol{s})$ is the kinematics that transforms the vector in the sensor coordinate to the one in the feedback coordinate. The final term $\boldsymbol{v}$ represents the internal force among wires.

The P control element given by Eq. (4) means the following steps on the sensor-actuator map.

$\boxed{\text{STEP 1}}$ Leading a path from the position of the end-effector node ($\boldsymbol{x}$) to the feedback coordinate. (That is $G_i(\boldsymbol{x_d})$ in Eq. (4).)

$\boxed{\text{STEP 2}}$ Leading another path from the sensor node to the feedback coordinate. (That is $G_j(\boldsymbol{s})$ in Eq. (4).)

$\boxed{\text{STEP 3}}$ Transforming the vector in the feedback coordinate into the corresponded force vector though the transfer arrow of proportion feedback.

$\boxed{\text{STEP 4}}$ Leading the path from the force vector in STEP 3 to the actuator node $\boldsymbol{\alpha}$.

Paths that can be leaded to the goal (that is the actuator node) through the steps imply realizable feedback control laws. Therefore inverse-transforming from transfer arrows to mathematical expression given by Eqs. (1) to (3) yields feedback control laws

As far as the D element of PID control is concerned, it can be obtained through almost the same steps of the P element. That is $\boxed{\text{STEP 2}}$ - $\boxed{\text{STEP 4}}$, omitting $\boxed{\text{STEP 1}}$,

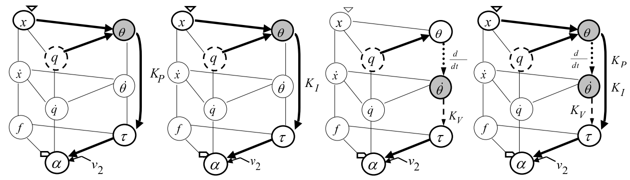

Figure 3. Example Paths of P, I, D Feedback Elements

because the desired vector $\dot{\boldsymbol{x}}_{\boldsymbol{d}}$ is set to zero. Finally, the remaining I element can be obtained through the same steps of P element.

Now, the overlap of P, I and D paths can express a PID control law on the sensor-actuator map. Moreover, by the transforming the PID paths to mathematical expression, and then by combining them, the PID control laws as actuator input can be obtained.

For example, when we obtain the paths shown in Fig. 3(a)-(c) as P, I and D elements, overlapping the paths yields Fig. 3(d) as the expression of PID control. (In the following, important nodes constructing feedback control the feedback node and the actuator node are accented visually.) Then, analytically inverse-transforming the combined path to mathematical expression yields the following equation as one of actuator input $\boldsymbol{\alpha_{PID}}$ in this case.

$$\begin{aligned} \boldsymbol{\alpha_{PID}} \;=\; & \boldsymbol{J_4^{+T}}(\boldsymbol{\theta})\Big[\boldsymbol{K_{P1}}\big(G_6(\boldsymbol{x_d}) - G_3(\boldsymbol{q})\big) \\ & -\boldsymbol{K_{V1}}\frac{dG_3(\boldsymbol{q})}{dt} + \boldsymbol{K_{I1}}\int_0^T \big(G_6(\boldsymbol{x_d}) - G_3(\boldsymbol{q})\big)dt\Big] \\ & +\boldsymbol{v_2}. \end{aligned} \tag{5}$$

Even though there are two kinds of transformation that means the $\boldsymbol{\tau} \rightarrow \boldsymbol{\alpha}$, $\boldsymbol{\alpha} = \boldsymbol{J_4}^{+T}(\boldsymbol{\theta})\boldsymbol{\tau} + \boldsymbol{v_2}$ is selected in this case. In the map, we also obtain plural paths as PID control laws on a sensor-actuator map. So, it is necessary to select excellent control laws from such plural PID control laws.

2.4 Selection of paths

The total numbers of control laws obtained from the map depends on the numbers of entered transfer arrows and sensors, then generally there exists many combinations of the arrows to compose PID control laws. In this subsection, we assume that all transformations among the vectors can be analytically calculated and the system can directly obtain $\boldsymbol{x}$, $\boldsymbol{\theta}$ and $\boldsymbol{\alpha}$ from displacement sensors as a case study. These vectors can be candidates for sensor nodes. Under such assumptions, the system has more than 8×10^6 combinations of PID feedback control laws. So, it is necessary to establish a sort of selection policy to narrow down the laws in order to employ actually. First, we consider the following initial setting for the purpose to select the basic control

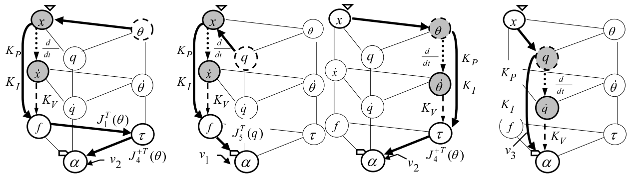

(I) (II) (III) (IV)

Figure 4. Selected PID Paths

laws.

$\boxed{\text{Initial Setting}}$ *P, I and D feedback are achieved in the same coordinate and utilize only one kind of sensor to measure* $\boldsymbol{x}$ *or* $\boldsymbol{q}$ *or* $\boldsymbol{\theta}$.

However, it might not be enough to narrow down control laws. Then, we should consider other selection policy to narrow down control laws as few as possible. From the viewpoint of the accuracy of positioning, qualitatively, less times of kinematics transformation is desirable since the error accumulation is less. Therefore, we establish the following selection policy.

$\boxed{\text{Selection Policy 1}}$ *The transformations from the sensor node into the feedback node is not achieved if the two nodes, the origin and the end, are the same. The transfer arrow can be employed one time if the two nodes are not the same. Also, transformation from the end-effector position node to the feedback node is in the same manner.*

Moreover we set the selection policy 2 to reduce the error in Jacobin matrices from the viewpoint of convergence time of the positioning and expansion for force control.

$\boxed{\text{Selection Policy 2}}$ *We can use only the Jacobian matrices in which displacement vectors can be measured directly from sensors.*

The above policies can narrow down the control laws, then finally we have nine candidate paths for PID control in this case.

2.5 Control Laws

We consider PID position control of the serial-link structure driven by parallel-wire mechanism introduced in subsection 2.1 as a case study. First, we investigate the realization of the transfer arrows in the system shown in Fig. 1. The system has all transfer arrows realized on the assumption that the diameter of links can be ignored and neighbor connect points of wires can be regarded as the same point. And the wire length node $\boldsymbol{q}$ or the joint angle $\boldsymbol{\theta}$ can be a sensor node on the map.

In this case, we obtain Fig. 4-(I) , (II), (III) and (IV), then also PID control laws are mathematically obtained as expressed by Eqs. (6) to (9).

Obtained from Fig. 4 (I)

$$\begin{aligned}\boldsymbol{\alpha_{PID}} &= \boldsymbol{J_{4(\theta)}}^{+T}\boldsymbol{J_1}(\boldsymbol{\theta})^T\Big[\boldsymbol{K_{P2}}\big(\boldsymbol{x_q}-G_1(\boldsymbol{\theta})\big)\\ &\quad -\boldsymbol{K_{V2}}\frac{dG_1(\boldsymbol{\theta})}{dt}+\boldsymbol{K_{I2}}\int_0^T\big(\boldsymbol{x_d}-G_1(\boldsymbol{\theta})\big)dt\Big]\\ &\quad +\boldsymbol{v_2}\end{aligned} \tag{6}$$

Obtained from Fig. 4 (II)

$$\begin{aligned}\boldsymbol{\alpha_{PID}} &= \boldsymbol{J_5}(\boldsymbol{q})^T\Big[\boldsymbol{K_{P2}}\big(\boldsymbol{x_d}-G_5(\boldsymbol{q})\big)-\boldsymbol{K_{V2}}\frac{dG_5(\boldsymbol{q})}{dt}\\ &\quad +\boldsymbol{K_{I2}}\int_0^T\big(\boldsymbol{x_d}-G_5(\boldsymbol{q})\big)dt\Big]+\boldsymbol{v_1}\end{aligned} \tag{7}$$

Obtained from Fig. 4 (III)

$$\begin{aligned}\boldsymbol{\alpha_{PID}} &= \boldsymbol{J_4}(\boldsymbol{\theta})^{+T}\Big[\boldsymbol{K_{P1}}\big(G_6(\boldsymbol{x_d})-\boldsymbol{\theta}\big)-\boldsymbol{K_{V1}}\frac{d\boldsymbol{\theta}}{dt}\\ &\quad +\boldsymbol{K_{I1}}\int_0^T\big(G_6(\boldsymbol{x_d})-\boldsymbol{\theta}\big)dt\Big]+\boldsymbol{v_2}\end{aligned} \tag{8}$$

Obtained from Fig. 4 (IV)

$$\begin{aligned}\boldsymbol{\alpha_{PID}} &= \boldsymbol{K_{P3}}\big(G_2(\boldsymbol{x_d})-\boldsymbol{q}\big)-\boldsymbol{K_{V3}}\frac{d\boldsymbol{q}}{dt}\\ &\quad +\boldsymbol{K_{I3}}\int_0^T\big(G_2(\boldsymbol{x_d})-\boldsymbol{q}\big)dt+\boldsymbol{v_3}\end{aligned} \tag{9}$$

We confirmed that the obtained control laws had the end-effector converge to the desired position through the positioning experiments, even though steady state errors existed.

3 Conclusion

We have proposed the sensor-actuator map for the organization of position sensor feedback control for multiple links structure / wire driven system. We have indicated that combining the transfer arrows and making paths on the map can express PID control, and also introduced the selection policies to narrow down the paths.

The selection policies of paths described in this paper are not used to find out the optimal control law. The study of selection policies to find out the quantitatively optimal control law is one of the most important future works.

References

[1] S.Hirose and S.Ma: Redundancy Decomposition Control for Multi-Joint Manipulator, *Proc. of IEEE Int. Conf. on Robotics and Automation*, pp.119-124, 1989.

[2] H. Kino, and S. Kawamura, "Development of A Serial Link Structure / Parallel Wire System for A Force Display", *Proc. of IEEE International Conference on Robotics and Automation*, MPI-6-3, 2002.

[3] S.Kawamura, H.Kino and W.Choe, "High speed manipulation by using parallel wire driven robots", *ROBOTICA, Cambridge University Press*, vol.18, part 1, January/February, pp.13-21, 2000.